CIRM 26
March 1999

NATIONAL PHYSICAL LABORATORY

Neutron response characteristics of the NPL tissue-equivalent proportional counter

by

G.C. Taylor
Centre for Ionising Radiation Metrology

Abstract

The aim of this work was to provide information which could be used to improve the accuracy with which tissue-equivalent proportional counters (TEPCs) measure dose equivalent. To this end the variation in TEPC dose equivalent with neutron energy has been determined using calculation and measurements. By comparing these values with the accepted values for ambient dose equivalent ($H^*(10)$), the efficiency of the TEPC for the measurement of $H^*(10)$ was determined over the energy range from thermal to 15 MeV. Analytical approaches for improving the $H^*(10)$ efficiency of the TEPC were then investigated.

ISSN 1369-6793

National Physical Laboratory
Teddington, Middlesex, UK, TW11 0LW

Approved on behalf of Managing Director NPL, by Dr Julian Hunt
Head, Centre for Ionising Radiation Metrology.

CONTENTS

1. INTRODUCTION

1.1 TEPCs and their use as dose equivalent meters

Low pressure tissue-equivalent proportional counters (TEPCs) are instruments which measure absorbed dose using a technique based on the Bragg-Gray cavity theory[1]. By keeping the filling pressure low, the energy loss of individual charged particles crossing the detector cavity corresponds to the energy loss in tissue over distances of the order of a few micrometres. The energy deposited in the chamber is usually expressed as a *lineal energy, y,* which is formally equal to the energy deposited in the cavity divided by the mean chord length of the cavity. Lineal energy therefore represents a track-averaged *Linear Energy Transfer, LET, or L.* The resulting spectrum consequently has regions that can clearly be identified as originating from specific recoil particles, as shown in Figure 1. The relationship between L and y means that the *radiation quality,* Q, can be assessed, using recommended Q(L) functions and making the assumption that y is approximately equal to L. Multiplying the value obtained for $\overline{Q}$ by the value for absorbed dose gives a value for a dose equivalent quantity, usually equated with the operational quantity Ambient Dose Equivalent, $H^*(10)$. However, the efficacy of the TEPC as a meter for $H^*(10)$ deteriorates rapidly below a few hundred keV, reflecting the differences between the TEPC and the artefact used in the definition of $H^*(10)$: the typical TEPC has TE plastic walls roughly 1 - 2 mm thick whereas $H^*(10)$ is defined at a point 10 mm below the surface of the 30 cm diameter ICRU sphere[2].

The TEPC response in terms of ambient dose equivalent (denoted R_H) varies considerably with energy, being ~60% at thermal energies, but falling to ~1% at 400 eV, before rising again to ~100% at higher energies (2 MeV and above), as can be seen in Figure 2. Clearly this means that the dose equivalent recorded by a TEPC in an environment with a soft neutron field will be considerably less than the ambient dose equivalent of that neutron field.

2. PREVIOUS RESULTS

Several laboratories have investigated approaches to improving the TEPC ambient dose equivalent response, but all have involved modifying the detectors themselves by increasing the wall thickness, reducing the filling pressure, altering the gas composition, or some combination thereof.[3-5] Each of these approaches has positive and negative aspects but, generally speaking, improving an instrument's ambient dose equivalent response in one energy region tends to degrade the response in other regions.

However, previous work published by NPL[6] reported on attempts to produce a weighting function F(y) as an alternative to Q(y). The new function was physically meaningless at any specific value of lineal energy but, when folded with a TEPC spectrum, gave a better estimate of ambient dose equivalent. The function was developed using an iterative procedure identical in concept to the back-error propagation techniques used to train neural networks. In fact, the function could be regarded as a linear neural network (i.e., one where the strength of the output from a neuron is directly proportional to that neuron's input).

The advantage of using a purely analytical method to improve R_H, the ambient dose equivalent response, of the TEPC is that the TEPC itself remains unaltered, hence there are no additional constraints on the experimental conditions under which it can be operated. Furthermore, the method can be performed retrospectively to measurements that have already been performed. Indeed the method was tested in just this way, using measurements for monoenergetic neutron beams performed at the German National Standards Laboratory, PTB and at NPL between 1986 and 1988.

In essence, the technique works as follows: a microdosimetric spectrum is selected and a

weighted sum of its bins is calculated. Initially, the weights are random, varying linearly between -1 and +1. This weighted sum is then compared to the desired ambient dose equivalent value, i.e., the value associated with the neutron field responsible for the microdosimetric spectrum. The difference between the desired $H^*(10)$ dose equivalent value and the weighted sum is then used as a multiplier to a small increment (known as the learning rate) applied to each weight, which is also multiplied by the content of the bin with which the weight is associated. The adjusted weights are then used to perform a weighted sum of a second microdosimetric spectrum, and the process repeated. The approach can be summarised in the following expression for the incremental weight change:

$$\Delta w(y) = \left(H^*(10)_{specX} \quad \Sigma_y\, w(y)\; y.d(y)_{specX}\right) \times y.d(y)_{specX} \times R_{learn}$$

In other words, the larger the discrepancy between the desired output ($H^*(10)$) and the network output ($\Sigma_y\, w(y)\; y.d(y)$) for a given microdosimetric spectrum ($specX$), the larger the correction that is fed back to the weight ($w(y)$), modified by the contents of the bin with which the weight is associated ($y.d(y)$). The learning rate (R_{learn}) acts as a brake on the learning process, allowing the network to approach its best set of weights in a controlled manner rather than oscillating wildly.

This learning process carries on, using a number of different spectra, known as the training set. Once all the spectra in the training set have been through the process, it returns to the first spectrum and starts again, continuing in this way until some convergence criterion is met. The greater the number of spectra in the training set, the more robust the solution should be.

The technique was applied to a training set of thirty theoretical microdosimetric spectra, generated by the computer code MITE60 (see section 4), but over a reduced range of lineal energies (10 - 1000 keV μm^{-1}). The lower limit was set to exclude the region of the spectrum containing the photon component, and the upper limit set because the number of spectra with components above this value was small. The training set covered the neutron energy range between 20 keV (representing the lowest neutron energy at which recoil protons would contribute to the lineal energy spectrum above 10 keV μm^{-1}) and 20 MeV (the upper limit of many of the neutron cross section data tables).

The network was tested using measured spectra, which were therefore independent of the training process, and the results were very encouraging. The TEPC dose equivalents determined using the alternative function varied from 90% to 130% of the ambient dose equivalent for eight monoenergetic neutron spectra from 24 keV up to 15 MeV, whose uncorrected values varied from 20% to 90% of the true ambient dose equivalent. Two broad-range 'realistic' spectra were also used in the test, one from a D_2O-moderated ^{252}Cf source and the other produced by the ASPIS facility at AEA Winfrith[7], which is no longer operational. Both spectra were corrected to within 5% of their true ambient dose equivalent values from measured dose equivalents of ~70%.

Although encouraging, the results fell far short of validating the technique due to the small number of test spectra. In addition, there were significant differences between the measured spectra and their theoretical counterparts. The measured spectra had been calibrated using the internal ^{244}Cm α-source, corresponding to a proton edge lineal energy value of roughly 145 keV μm^{-1}, as opposed to the value of 120 keV μm^{-1} being predicted by the TEPC code. Furthermore, the predicted spectra had, on the whole, significantly smaller proton components.

The former problem was dealt with by redefining the position of the measured spectras' proton edge positions to equal that of the theoretical spectra. Fortunately, this simply entailed shifting the measured spectra by five bins due to the logarithmic nature of the lineal energy axis, although this then necessitated a reevaluation of the measured values for the doses and quality factors, and hence the dose equivalents.

The latter problem (that of significantly smaller proton components) was thought to be due to the limitations of the model employed in generating the theoretical spectra. A particle's energy loss in the gas was calculated using the continual slowing down approximation, and that energy was assumed to be deposited locally, i.e., in the gas. Furthermore, secondary interactions caused by neutrons scattered within the detector were ignored due to pressures of computer time, and it was this last limitation that was thought to be most significant.

3. THE AIM OF THE PROJECT

Despite the limitations of the theoretical training set used in the earlier work, and the limited number of measured spectra used to test the correction technique, the results were still very encouraging and merited further investigation. The aim of this project was therefore to build upon this earlier work by enhancing the models used to generate the theoretical training set, to investigate other potential methods for correcting the TEPC dose equivalent measurements, and to evaluate them using a much wider set of test spectra.

4. THE TEPC MODELLING PROGRAM MITE60

The TEPC Monte Carlo code MITE60 (microdosimetry in important tissue elements below 60 MeV) was originally developed at the University of Birmingham[8], but has been revised and updated in many ways in recent years. Essentially, the program models the tissue equivalent wall and gas filling of a TEPC, tracking the products of neutron interactions (both neutral and charged particle recoils) as they traverse the counter. Neutral particles are forced into subsequent collisions along their path until either captured or their weighting factor falls below a predetermined threshold. Should a secondary charged particle enter the sensitive volume of the detector, the program calculates the energy lost in the gas and bins the event accordingly.

The code was originally validated by comparison with other codes such as NESLES[9,10], and has been used to calculate carbon kerma values up to 60 MeV[8], using the cross section data of ENDF/B IV, Brenner and Prael[11], Dimbylow[12], Islam *et al.*[13] and Meigooni *et al.*[14].

In order to improve the realism of the model, several new features have been included in the code:

- Proton radial energy distribution: this determines if any energy is lost non-locally (i.e. outside the cavity) due to the finite radius of the ionisation track (usually only important for higher energy protons)[15],
- Proton energy straggling: taken from Wilson *et al.*[16], this allows for the statistical nature of energy deposition in small volumes, and

  W-value curves: taken from Siebert *et al.*[17] (^{1}H) and Taylor *et al.*[18] (^{4}He, ^{12}C, ^{14}N, ^{16}O), this allows for the increasing energy required to create ion pairs at lower particle energies.

Similarly, the data used by the code has been updated:

Neutron cross sections from ENDF/B VI, and

Proton and alpha-particle stopping powers and ranges from ICRU 49[19] (other stopping powers and ranges are still taken from Ziegler[20]). An important consequence of the new stopping powers was a change in the theoretical proton edge position from 120 keV μm^{-1} to 136 keV μm^{-1}.

With the development of faster, more powerful and more widely available computers, the tracking of the secondary neutron interactions has become much easier and can now be performed as a matter of course. Combined with the above modifications, much better agreement between the model and experiment were expected.

5. THE MONOENERGETIC MEASUREMENT PROGRAMME

A new set of monoenergetic measurements were performed in the low-scatter facility at NPL at the following ISO-recommended[21] energies: 144 keV, 250 keV, 565 keV, 1.2 MeV, 2.5 MeV and 5.0 MeV. The scatter contribution in each case was accounted for using the shadow cone method. Each spectrum was collected in three simultaneous gain runs using linear spectroscopy amplifiers with gains incrementing by a factor of ten. The amplified pulses were then fed into three PC-based MCA cards. Absolute calibration of the spectra was based on the proton edge method, which as mentioned above, was now assumed to be at a value of 136 keV μm^{-1}. The three linear pulse height spectra were converted into a single logarithmic dose spectrum using software written and tested at NPL.

The results are shown normalised to unit fluence in Figure 3, and are compared to experimental results obtained using the counter at PTB and at NPL in previous years. It can be seen that, in general, the agreement is reasonable, apart from the expected displacement in the proton edge. The only other differences worthy of comment are to be seen in Figures 3(d) and 3(e), i.e., the two highest energies. At 2.5 MeV, there seems to be a small difference in normalisation, with the 1996 NPL results being approximately 10% higher than the 1987 PTB result. At 5 MeV, however, the slightly different shapes appears to be due to the poor resolution of the 1987 NPL measurement, indicating that the counter may have been operated at an above-optimal voltage.

6. MODELLING THE TEPC USING MITE60

As outlined in Section 4, the TEPC code MITE60 models the tissue-equivalent wall and filling gas of a microdosimetric counter, tracking both charged and neutral secondary particles. The secondary charged particles are tracked as they slow down and, if they enter the cavity of the detector, the amount of energy deposited there is recorded. The secondary neutral particles are forced into further collisions until either they undergo capture or their forced-collision weighting factor falls below a cutoff level.

Initially, the TEPC was modelled with the accepted compositions for wall and gas material: i.e., H (10.2%), C (76.8%), N (3.6%), O (9.4%, which includes the F and Ca contributions of 1.7% and 1.8% respectively)[22]. However, on comparing the results with experiment (Figure 4), the agreement was disappointing, showing similar discrepancies to those observed with the original model. The reason for these discrepancies still appeared to be a lack of proton recoils from the wall material, given the reasonable agreement at lower energies which gets progressively worse (c.f., gas events accounting for ~60%, ~45%, ~20%, ~12%, ~7% and ~4% of the dose at 144 keV, 250 keV, 565 keV, 1.2 MeV, 2.5 MeV and 5.0 MeV respectively). This observation is also backed up by comparing the measured and predicted heavy ion

components (above 136 keV μm^{-1}) for the spectra at 2.5 and 5.0 MeV, which show good agreement.

The apparent excess of hydrogen in the real counter could be due to several causes, but these fall into two categories: either anomalies within the detector or problems with the modelling code. On the detector side, the tissue-equivalent plastic used in constructing the counter could be deficient in graphite, or the presence of hydrogen-rich field pieces could be contributing to the detector response. On the modelling side, it is possible, although unlikely, that there is a bug in the code that affects the proton energy deposition (as the magnitude of the heavy recoil components at the higher energies looks reasonable). Studying the results of previous measurement intercomparisons[23], the first explanation appears more likely, as the results for the ambient dose equivalent response for this specific TEPC are significantly higher when compared to other TEPCs of similar construction. This implies that the oddity is specific to this TEPC. Unfortunately, short of dismantling and analysing the detector (and thereby destroying it), there is no way to verify this conclusion.

Regardless of the cause of this anomaly, increasing the hydrogen component of the TEPC wall material in the model from 10.2% by weight to 14.0% improves the agreement between the measurements and the calculations significantly, as shown in Figures 5. Although much improved, the agreement is still not perfect, as demonstrated at lower lineal energies for the 2.5 MeV and 5.0 MeV spectra. This is thought to be caused by limitations in the straggling model used, and will be investigated in the 1998 - 2001 NMS Ionising Radiation Metrology programme.

The improvement in the agreement between the measured and predicted spectra meant that it became possible to create a theoretical TEPC response matrix, from thermal energies to 15 MeV, which could be used to help interpret the shape of spectra measured in the field with a view to assessing the degree of under-read present in the dose equivalent measurement. A three-dimensional plot of the response function can be seen in Figure 6, which shows how the shape and magnitude of the calculated microdosimetric spectrum changes with neutron energy.

7. TECHNIQUES FOR CORRECTING THE DOSE EQUIVALENT UNDER-READ

Four techniques were investigated to assess their potential for correcting the poor ambient dose equivalent response of the TEPC to neutron spectra with significant numbers of low/intermediate energy neutrons:

- An alternative weighting factor to the Q(y) relationship normally used,
- A pattern-recognition neural network that can estimate the degree of under-response from the shape of the microdosimetric spectrum,
- Mean-value matching, where the frequency-mean and/or dose-mean lineal energy values of the spectra in question are compared to those of the theoretical monoenergetic spectra, the most closely matched spectrum yielding a value for the dose equivalent under-read, and

  Spectrum matching, where the microdosimetric spectra in question are compared to the theoretical spectra for monoenergetic neutron irradiation using residual-sum-of-squares, the most closely matched theoretical spectrum yielding a value for the dose equivalent under-read.

In order to test the techniques more thoroughly, an expanded set of test spectra was created. This set was divided into four groups: the monoenergetic measurements performed as part of the 1995-1998 programme (144 keV - 5 MeV), monoenergetic measurements performed during the 1986-1989 programme (24 keV - 5 MeV)[23,24], measurements performed for broad range neutron spectra during previous programmes (1986-1995)[7,25-27], and spectra synthesised using the theoretical response matrix for a selection of workplace fields held in the neutron spectrum catalogue SPKTBIB[28].

The microdosimetric spectra derived from the SPKTBIB catalogue were divided into 7 categories: transport flasks (7 spectra), MOX fuel storage (2 spectra), radionuclide neutron source fabrication (5 spectra), WWR fuel (4 spectra), transuranium element processing (5 spectra), fuel processing (7 spectra) and gas-cooled reactors (9 spectra).

The techniques and their results are explained in more detail below.

7.1 Alternative Weighting Factor (Linear Network)
As explained in Section 1, this approach uses the back-error propagation techniques for training neural networks. Randomly generated weights were incremented in order to iterate the predicted value for ambient dose equivalent response, R_H, towards the true value for R_H for a series of 51 training spectra, from 20 keV to 15 MeV. No spectra were included below 20 keV as the only component of these spectra that would be visible above a lineal energy of 10 keV μm^{-1} would be from the $^{14}N(n,p)$ reaction, and all would have essentially the same shape. Given the range of R_H values associated with neutrons with energies between thermal and 20 keV, this was thought to be inappropriate. The training was considered complete when all of the predicted values for R_H were within 0.05 of the actual value. In this case it took approximately 4×10^5 iterations. The resulting weight distribution is shown in Figure 7. Surprisingly, the distribution looks almost random, having no real consistency apart from all being positive above 700 keV μm^{-1}. Nevertheless, the predicted values for R_H are generally good, as shown in Figure 8.

As can be seen in Figure 8a, the correction to the R_H values for the recent monoenergetic measurements is significant at lower neutron energies, but overcompensates at higher energies, especially at 2.5 MeV. Nevertheless, taken overall, the corrected answers are more consistent: the range of the uncorrected R_H values is 0.616 to 1.008, whereas for the corrected values it is 0.835 to 1.213. The two means and associated standard deviations are (0.86 ±0.17) and (1.05 ±0.13) respectively.

Similarly, in Figure 8b, the correction to the R_H values for the previous monoenergetic measurements are similar to those outlined above: the uncorrected values range from 0.289 to 1.150, whereas the corrected values range from 0.721 to 1.087. The means and associated standard deviations are (0.78 ±0.31) and (0.93 ±0.14) respectively.

In Figure 8c, the correction to the R_H values for the broad-spectrum measurements are again similar to those outlined above: the uncorrected values range from 0.653 to 0.980, whereas the corrected values range from 0.809 to 1.216. The means and associated standard deviations are (0.87 ±0.13) and (0.99 ±0.15) respectively.

The interpretation of Figure 8d, however, is rather more problematic. In general the corrected values are very good; however, this is not surprising as the microdosimetric spectra under test have been synthesised from the monoenergetic spectra in the theoretical response matrix. The discrepancy lies in the Gas-Cooled Reactor (GCR) group: these values have not been corrected particularly well (although there is a significant improvement in all cases), which indicates that it will be necessary to incorporate thermal energy spectra into the training set in order for the training regime to take account of the spectra at energies below 20 keV.

However, it will probably be necessary to use an artificially low R_H value for the thermal spectra in the training set in order to allow for the very poor dose equivalent response of the TEPC in the low keV energy range, because of the similarity in the shape of low keV microdosimetric responses to that at thermal energies.

Nevertheless, the corrected answers are an improvement: the uncorrected values range from 0.333 to 0.906, whereas the corrected values range from 0.408 to 0.994. The means and associated standard deviations are (0.71 ±0.17) and (0.88 ±0.16) respectively.

7.2 Pattern Recognition (Sigmoid) Network

The use of an orthodox sigmoid neural network in the determination of the TEPC dose equivalent under-read was thought to have promise because of their well-known pattern-recognition abilities. In contrast to a 'linear' neural network used to generate an alternative function to the established Q(L) relationship, an 'orthodox' neural network uses a sigmoid-shaped function to communicate between layers. This is supposed to mimic the way that nerve cells react to stimuli from other nerve cells (or neurons). A useful introduction to neural networks, including training regimes, can be found in Dayhoff[29].

Essentially, a sigmoid function is a 'blurred' step function, of the form

$$f(x) = \frac{1}{1 + e^{-x}}$$

This has close to a zero value for x < -5, a value of roughly unity for x > +5 and is equal to 0.5 when x equals zero. In this case, x, represents the weighted sum of the inputs to the neuron, and f(x) the neuron's output.

Put simply, an enormous value input into a linear network's neuron would be scaled up or down, but the neuron's output would always be proportional to its input. Conversely, a sigmoid network's neuron's output has a maximum value, which is approached asymptotically.

The sigmoid network used in this case consisted of three layers, known as the input, hidden and output layers, comprising 110 neurons, 3 neurons and 1 neuron respectively. Each neuron in the input layer is connected to each neuron in the hidden layer, and each neuron in the hidden layer is connected to the single output neuron. The network was trained in an analogous manner to the linear network, being trained between the neutron energies from 20 keV to 15 MeV using back-error propagation, although the expressions for calculating the weight increments were rather more complex. The network was allowed to train for ~4000 iterations and then tested as with the linear network outlined above, the results being shown in Figure 9.

As can be seen in Figure 9a, the correction to the R_H values for the recent monoenergetic measurements is reasonable at lower neutron energies, but again, overcompensates at higher energies, especially at 1.2 and 2.5 MeV. Nevertheless, taken overall, the corrected answers are better: the range of the uncorrected R_H values is 0.616 to 1.008, whereas for the corrected values it is 0.905 to 1.244. The two means and associated standard deviations are (0.86 ±0.17) and (1.09 ±0.14) respectively.

Surprisingly, in Figure 9b, the correction to the R_H values for the previous monoenergetic measurements is very poor: the network has not recognised the two low energy points for what they are and has therefore underestimated the correction factors. Nevertheless, it has improved the results, albeit only marginally: the uncorrected values range from 0.289 to

1.150, whereas the corrected values range from 0.303 to 1.281. The means and associated standard deviations are (0.78 ±0.31) and (0.95 ±0.34) respectively.

In Figure 9c, the correction to the R_H values for the broad-spectrum measurements are reasonably good: the uncorrected values range from 0.653 to 0.980, whereas the corrected values range from 0.805 to 1.114. The means and associated standard deviations are (0.87 ±0.13) and (1.01 ±0.12) respectively.

The interpretation of Figure 9d, however, is reminiscent of the linear network. In general, the corrected values are very good; however, given the way these TEPC responses were generated, this is to be expected. Again, the discrepancy lies in the Gas-Cooled Reactor (GCR) group: these values have not been corrected very well, and adds weight to the argument that predicted microdosimetric spectra at thermal neutron energies need to be included in the training process. The overall improvement is, however, clear: the uncorrected values range from 0.333 to 0.906, whereas the corrected values range from 0.524 to 1.070. The means and associated standard deviations are (0.71 ±0.17) and (0.91 ±0.16) respectively.

7.3 Mean-Value Matching

The technique of mean-value matching assumes that the mean dose deposited per event (above 10 keV μm^{-1}) will be similar for microdosimetric spectra with similar R_H values. However, as can be seen in Figure 10, the frequency-mean lineal energy values for the theoretical monoenergetic TEPC responses vary with R_H in such a way that no unique value of R_H may be assigned to quite large ranges of $\bar{y}_f$. The relationship between $\bar{y}_f$ and R_H is, however, explicable in terms of the underlying physics when considering how both parameters vary with neutron energy, as can be seen in Figure 11, which also shows the R_H curve of Nunes and Waker from Figure 2. In general, the agreement between the two predictions for R_H is reasonable: the only real region of disagreement is between 1 keV and 100 keV, and may be due to the simplicity of the MITE60 model (i.e., just the A150 TE spherical shell and filling gas), or to simplifications in Nunes and Waker's analytical fit.

At thermal neutron energies, the $^{14}N(n,p)^{14}C$ reaction dominates the TEPC response; however, the presence of boron contamination in the A150 plastic can result in a contribution from the $^{10}B(n,\alpha)^{7}Li$ reaction. This contribution differs from detector to detector, as the amount of boron contamination in A150 plastic does vary from batch to batch. Smathers *et al.*[22] analysed two samples of A150 plastic: one contained 3.4 ppm natural boron by weight, the second < 2.0 ppm (their limit of detection). Furthermore, it would only take approximately 10 ppm of natural boron by weight in order to match the TEPC response from the nitrogen component in A150. These exo-ergic reactions generate relatively high energy charged particles that deposit energy in the TEPC cavity in a manner indistinguishable from endo-ergic reactions that produce particles of similar energies, leading to reasonably high values for the $\bar{y}_f$, and also for R_H (~0.5, assuming zero boron content, higher if boron is present). The fact that the R_H value for a TEPC with boron-free A150 plastic is not closer to unity is caused by the lack of moderating material in the TEPC, which cannot therefore generate and degrade the 2.2 MeV photons created from hydrogen capture, as happens in an object having the bulk of the ICRU sphere.

There is evidence to show that the boron contamination of the NPL 5" TEPC is low, although non-zero. A thermal measurement was performed as part of the 1986-1989 programme, although the upper limit for this measurement seems to have been set at ~300 keV μm^{-1} [30], probably because no events were expected above the proton edge. Consequently, only part of the α-component from the boron contamination is present, and this is the reason for the spectrum being left out of the old monoenergetic measurement test set.

At epithermal and lower intermediate neutron energies, a steady decline in R_H is observed,

as the number of neutrons being thermalised falls due to lack of moderating material; it only starts to recover once the response from the endo-ergic reactions starts to become significant, from ~1 keV upwards. The $\bar{y}_f$ value, however, remains reasonably constant up to ~10 keV, as the TEPC spectrum above 10 keV μm^{-1} is still only registering events from exo-ergic reactions. For neutron energies above 10 keV, the rapidly increasing response from hydrogen scatter soon dominates the shape of the spectrum, causing a rapid fall in the $\bar{y}_f$ value.

As the neutron energy is increased further, the R_H value increases as the effects of neutron moderation and attenuation in the ICRU sphere become less important. This makes the differences between the ICRU sphere and the significantly less massive TEPC less important. The fact that the $\bar{y}_f$ value starts to fall above ~600 keV is caused by the proton stopping power decreasing with increasing neutron energy, which dominates the observed trends until ~5 MeV, where the heavy recoil contribution to the TEPC spectrum starts to become significant, and offsets the fall in $\bar{y}_f$ driven by the falling proton stopping power.

The relative shapes of the R_H and $\bar{y}_f$ curves means that it is impossible simply to associate a value of R_H to each value of $\bar{y}_f$. The technique therefore requires another parameter to help establish which of a number of possible R_H values is the most appropriate for a particular $\bar{y}_f$. One such parameter is the fractional dose deposited above a lineal energy of 136 keV μm^{-1}, *i.e.*, the maximum energy that a proton can deposit in the counter. This helps separate the $\bar{y}_f$ values into distinct groups, as shown in Figure 12. This shows that all the monoenergetic values below an R_H of 0.85 have between 0 and 1% of their dose above 136 keV μm^{-1}. For R_H values between 0.2 and 0.85, most of the values fall on a reasonably smooth curve with the exception of three points clustered at R_H=~0.5, $\bar{y}_f$=~58, which are the three thermal points, and three others, two of which are 1 eV points, the third a 10 eV point. For those points above an R_H of 0.85, there are three with a high lineal energy dose fraction between 0 and 1%, but still having $\bar{y}_f$ values greater than 50 keV μm^{-1}. All other points above an R_H of 0.85 have larger high lineal energy dose fractions, and show a reduction in $\bar{y}_f$ value as that dose fraction increases. If it can be assumed that no workplace field will be of sufficiently low mean energy that the thermal component of the TEPC response will dominate the dose deposition (which is clearly contentious), then a reasonably simple scheme can be employed to determine the degree of TEPC under-response given the $\bar{y}_f$ value and the dose fraction above 136 keV μm^{-1}:

For spectra with dose fractions above 136 keV μm^{-1} between 0 and 1%, a fit to the relevant data can be employed,

For spectra with dose fractions above 136 keV μm^{-1} between 1 and 4%, a dose equivalent under-read of R_H equal to 0.9 may be assumed, necessitating a correction of ×1.11, and

For spectra with dose fractions above 136 keV μm^{-1} of 4% or more, no correction is necessary.

Figure 13 shows the results of employing this corrective scheme.

As seen in Figure 13a, the correction to the R_H values for the recent monoenergetic measurements is extremely good: the range of the uncorrected R_H values is 0.616 to 1.008, whereas for the corrected values it is 0.953 to 1.079. The two means and associated standard deviations are (0.86 ±0.17) and (1.014 ±0.049) respectively.

Similarly, in Figure 13b, the correction to the R_H values for the previous monoenergetic measurements show good improvements: the uncorrected values range from 0.289 to 1.150, whereas the corrected values range from 0.924 to 1.202. The means and associated standard deviations are (0.78 ±0.31) and (1.07 ±0.11) respectively.

In Figure 13c, the approach of leaving the TEPC value for the dose equivalent unchanged for spectra with dose fractions above a lineal energy of 136 keV μm^{-1} of over 4% means that all but one point in the broad-spectrum measurements data set were left unaltered. As a result, the (completely) uncorrected values range from 0.653 to 0.980, whereas the unaltered/corrected values range from 0.726 to 0.980. The means and associated standard deviations are (0.87 ±0.13) and (0.89 ±0.10) respectively.

The results shown in Figure 13d, however, show a marked level of scatter. The bulk of the corrected values fall between 0.9 and 1.1, but again the values for the Gas-Cooled Reactor group are disappointing. The corrected answers are, however, still an improvement: the uncorrected values range from 0.333 to 0.906, whereas the corrected values range from 0.445 to 1.089. The means and associated standard deviations are (0.71 ±0.17) and (0.89 ±0.15) respectively.

7.4 Microdosimetric Spectrum-Matching

This approach is probably the most intuitively obvious: the microdosimetric spectra under test are normalised to the area under the curve above 10 keV μm^{-1} (to avoid the photon component), and then compared to each (similarly normalised) member of the theoretical response matrix, by calculating the residual sum-of-squares (RSOS) for each bin above 10 keV μm^{-1}. The theoretical spectrum with the lowest RSOS is then taken to be representative of the spectrum under test, including the theoretical value for R_H. Again, the predicted values for R_H are generally good, as shown in Figure 14.

As seen in Figure 14a, the correction to the R_H values for the recent monoenergetic measurements is generally very good: the range of the uncorrected R_H values is 0.616 to 1.008, whereas for the corrected values it is 0.951 to 1.107. The two means and associated standard deviations are (0.86 ±0.17) and (1.027 ±0.062) respectively.

Similarly, in Figure 14b, the correction to the R_H values for the previous monoenergetic measurements show similar improvements: the uncorrected values range from 0.289 to 1.150, whereas the corrected values range from 0.996 to 1.192. The means and associated standard deviations are (0.78 ±0.31) and (1.099 ±0.062) respectively.

In Figure 14c, the correction to the R_H values for the broad-spectrum measurements are again similar: the uncorrected values range from 0.653 to 0.980, whereas the corrected values range from 0.925 to 1.042. The means and associated standard deviations are (0.87 ±0.13) and (0.958 ±0.048) respectively.

The results shown in Figure 14d, however, again show a marked level of scatter. The improvement is still evident, with the bulk of the corrected values falling between 0.9 and 1.2, but yet again the values for the Gas-Cooled Reactor group are disappointing. In this case, the uncorrected values range from 0.333 to 0.906, whereas the corrected values range from 0.407 to 1.225. The means and associated standard deviations are (0.71 ±0.17) and (0.90 ±0.21) respectively.

7.5 Comparison of Techniques

Figure 15 compares the four correction techniques directly, and shows that there are no consistent trends. One observation, however, is that the sigmoid network is frequently at the extremes of the corrected values, whether it be high or low. The performance of the techniques can perhaps be best judged by comparing the means and standard deviations of the corrected answers for the four techniques. as summarised in the following Table:

	Linear Network	Sigmoid Network	Mean Matching	Spectrum Matching
New Mono Mmts	1.05 ±0.13	1.06 ±0.14	1.014 ±0.049	1.027 ±0.062
Old Mono Mmts	0.93 ±0.14	0.95 ±0.34	1.07 ±0.11	1.099 ±0.062
Spec Mmts	0.99 ±0.15	1.01 ±0.12	0.89 ±0.10	0.958 ±0.048
SPKTBIB	0.88 ±0.16	0.91 ±0.17	0.89 ±0.15	0.90 ±0.21
All Mmts	0.99 ±0.14	1.01 ±0.23	1.00 ±0.11	1.036 ±0.080

Overall, the results are surprisingly consistent and, at first glance, there seems little to distinguish the four techniques. However, if the measurement data are considered without the SPKTBIB data, then the spectrum-matching technique produces the most *precise* answers, inasmuch as the standard deviations are considerably smaller than for the other approaches. Conversely, the sigmoid network has consistently large standard deviations, and its failure to recognise the 24 keV point in the old monoenergetic measurement data set stands out significantly. The mean-matching technique performed well, given the added complication of using the dose fraction above a lineal energy of 136 keV μm^{-1} as a secondary parameter.

The results for the SPKTBIB data set are difficult to interpret given their creation from the data sets used to derive the correction techniques, but they can still act as useful guides to the performance of the TEPC with or without any corrections. Clearly the most worrying set from the SPKTBIB data is the Gas Cooled Reactor grouping. None of the techniques coped well at all, and more effort will be required to resolve this problem. The spectrum-matching technique produced five corrected dose equivalents that were 15% higher than the other techniques, but at worst overcompensated by less than 25%, and only two of these were worse than the uncorrected values.

Significantly, had the high lineal energy dose fraction technique been applied to the other approaches as well as the mean-value matching technique (where its application was essential), a number of the oddities highlighted earlier would have been improved:

Spectrum-matching: the five points 15% higher than the other approaches in the SPKTBIB data set featured in Figure 15d all had high lineal energy dose fractions between 1% and 4% and would consequently have been assigned a corrective R_H value of 0.9, identical to the values assigned by the mean-matching technique. Also, the point in the GCR set that was hardly corrected (R_H = 0.442, Dose > 136 keV μm^{-1} = 0.3%) had been matched with the 2.5 MeV monoenergetic (R_H = 0.941 Dose > 136 keV μm^{-1} = 3.42%, RSOS = 2.43×10^{-3}), yielding a corrected R_H value of 0.470, but with a clear mismatch in the high LET doses. However, the next best match was at 200 keV (R_H = 0.697, dose > 136 keV μm^{-1} = 0.0%, RSOS = 2.59×10^{-3}), which would provide a corrected R_H value of 0.634, which at least increases the level of correction.

Sigmoid network: the single contentious point for this technique was at 24 keV for the old monoenergetic measurement data set, which had a Dose > 136 keV μm^{-1} of 0.0%. However, the network identified this point as reasonably high energy, with an estimated R_H value of ~0.95, and the lowest Dose > 136 keV μm^{-1} for any spectrum with an R_H greater than 0.90 was 0.6%. Although this information could not be used to improve the correction, it would at least point out this inconsistency.

However, this merely represents the positive side of applying the extra technique; several answers in each of the other techniques would be worsened using this approach, and therefore further evaluation of its benefits will be necessary.

8. CONCLUSIONS

An improved theoretical response matrix of TEPC spectra for monoenergetic neutrons has been created, albeit using an increased hydrogen component for the A150 tissue-equivalent plastic. The ambient dose equivalent responses (R_H) derived from these spectra compare reasonably well with those published by Waker[31], and show just how poor the R_H values are at intermediate neutron energies.

Four techniques that correct for the poor R_H values at these energies have been investigated. All show improvements over the uncorrected values, with one or two significant exceptions. None of the four techniques coped with correcting the theoretical TEPC spectra from gas-cooled reactors (whose R_H values varied from 0.333 to 0.544), the best correction being achieved by the linear network, which corrected the 0.544 value to 0.818. This failure by all the approaches is thought to be caused, at least in part, by the limited number of spectra (and their poor statistics) in the response matrix below 1 keV. In the case of the two neural network approaches, this would result in a lack of training to recognise low energy spectra. For the spectrum-matching technique, this means fewer low energy spectra for comparison, and poor statistics means that the chances of a low residual sum-of-squares are small. The mean-matching technique would struggle due to large uncertainties in the $\bar{y}_f$ values, and also with large variations in the dose fraction above 136 keV μm^{-1}.

Currently, there is little to choose between the four techniques; in fact taking the mean of the four corrected values would reduce the impact of the occasional aberrant result. It is, however, imperative that the poor showing of all approaches for the gas-cooled reactor spectra be investigated. Initially, this may be achieved by bolstering the low energy part of the TEPC spectrum response matrix. This in itself may show one approach to be superior to the rest. If improving the response matrix does not help improve the corrections, the TEPC spectra generated from SPKTBIB data could be used to redevelop the techniques, acting as a training set for the neural network approaches and as reference data for the two matching techniques. If little improvement is achieved even then, it may be necessary to isolate the thermal part of the TEPC spectrum by performing matched measurements with and without cadmium shielding.

Clearly more measured spectra are required to help test the correction techniques, especially those containing lower energy neutrons. To this end a measurement in the NPL thermal column would be helpful. Furthermore, following the determination of the scatter characteristics of the NPL low scatter facility[32], a number of source-based measurements with and without shadow cone would provide TEPC spectra with substantial lower energy neutron components that have well-characterised fluence spectra.

Acknowledgements

This work was funded by the UK National Measurement System Policy Unit and was Deliverable (iv) of Project 3.6 in its 1995 to 1998 Programme for Ionising Radiation Monitoring Metrology. The title of the project was: *Report on the comparison between calculated and measured results and documentation of a definitive set of scatter components in support of the calibration of personal dosemeters and area survey instruments.*

REFERENCES

[1] FANO, U. Note on the Bragg-Gray cavity principle for measuring energy dissipation. *Radiat. Res.* 1954, 1, 237-240.

[2] International Commission on Radiation Units and Measurements, *Determination of Dose Equivalents Resulting from External Radiation Sources.* ICRU Report 39, 1983.

[3] EDWARDS, A.A. Low Pressure Proportional Counters in Radiation Protection. Improvements to Energy Response and Sensitivity. *Radiat. Prot. Dosim.*, 1989, 29(1-2), 109-112.

[4] PIHET, P., MENZEL, H.G., ALBERTS, W.G. and KLUGE, H. Response of Tissue-Equivalent Proportional Counters to Low and Intermediate Energy Neutrons using Modified TE-^{3}He Gas Mixtures. *Radiat. Prot. Dosim.*, 1989, 29(1-2), 113-118.

[5] GERDUNG, S., GRILLMAIER, R.E., LIM, T., PIHET, P., SCHUHMACHER, H. and SEGUR, P. Performance of TEPCs at Low Pressures: Some Attempts to Improve Their Dose Equivalent Response in the Neutron Energy Range from 10 keV to 1 MeV. *Radiat. Prot. Dosim.*, 1994, 52(1-4), 57-59.

[6] TAYLOR, G.C. An Analytical Correction for the TEPC Dose Equivalent Response Problem. *Radiat. Prot. Dosim.*, 1995, 61(1-3), 67-70.

[7] MURPHY, M.F. and SCOTT, M.C. *A Neutron Spectrometry and Dosimetry Intercomparison in the ASPIS Reference Fields, AEA Winfrith, Undertaken by Members of EURADOS Working Group 7.* Draft Report, November 1995.

[8] TAYLOR, G.C. and SCOTT, M.C. A Microdosimetric Monte Carlo Code for Neutrons up to 60 MeV. *Radiat. Prot. Dosim.*, 1992, 44(1-4), 53-56.

[9] EDWARDS, A.A. and DENNIS, J.A. *NESLES - A Computer Program which Calculates Charged Particle Spectra in Materials Irradiated by Neutrons.* NRPB Report M-43, 1979.

[10] TAYLOR, G.C. *The Prediction and Measurement of Microdosimetric Spectra Relating to Neutron Cancer Therapy.* PhD Thesis, University of Birmingham, 1990.

[11] BRENNER, D.J. and PRAEL, R.E. Calculated Differential Secondary-Particle Production Cross Sections after Nonelastic Neutron Interactions with Carbon and Oxygen between 15 and 60 MeV. *Atomic Data and Nuclear Data Tables*, 1989, 41(1), 71-130.

[12] DIMBYLOW, P.J. *Calculation of Neutron Cross-Sections for the Elements Hydrogen, Carbon, Nitrogen and Oxygen in the Energy Range 20 - 50 MeV.* NRPB Report R78, 1978.

[13] ISLAM, M.S., FINLAY, R.W., PETLER, J.S., RAPAPORT, J., ALARCON, R. and WIERZBICKI, J. Neutron Scattering Cross Sections and Partial Kerma Values for Oxygen, Nitrogen and Calcium at $18 < E_n < 60$ MeV. *Phys. Med. Biol.*, 1988, 33(3), 315-328.

[14] MEIGOONI, A.S., PETLER, J.S. and FINLAY, R.W. Scattering Cross Sections and Partial Kerma Factors for Neutron Interactions with Carbon at $20 < E_n < 65$ MeV. *Phys. Med. Biol.*, 1984, 29(6), 643-649.

[15] International Commission on Radiation Units and Measurements, *Microdosimetry.* ICRU Report 36, 1983.

WILSON, W.E., METTING, N.F. and PARETZKE, H.G. Microdosimetric Aspects of 0.3 - 20-MeV Proton Tracks: I. Crossers. *Radiat. Res.*, 1988, 115, 389-402.

SIEBERT, B.R.L., GRINDBORG, J.E., GROßWENDT, B. and SCHUHMACHER, H. New Analytical Representation of W Values for Protons in Methane-Based Tissue-Equivalent Gas. *Radiat. Prot. Dosim.*, 1994, 52(1-4), 123-127.

TAYLOR, G.C., JANSEN, J.T.M., ZOETELIEF, J. and SCHUHMACHER, H. Neutron W Values in Methane-Based Tissue-Equivalent Gas up to 60 MeV. *Radiat. Prot. Dosim.*, 1995, 61(1-3), 285-290.

International Commission on Radiation Units and Measurements, *Stopping Powers and Ranges for Protons and Alpha Particles.* ICRU Report 49, 1993.

ZIEGLER, J.F., BIERSACK, J.P. and LITTMARK, U. *The Stopping Power and Range of Ions in Solids.* Pergamon Press, Oxford, 1985.

International Organisation for Standardisation, *Neutron reference radiations for calibrating neutron-measuring devices used for radiation protection purposes and for determining their response as a function of neutron energy,* International Standard ISO 8529, 1989.

SMATHERS, J.B., OTTE, V.A., SMITH, A.R., ALMOND, P.R., ATTIX, F.H., SPOKAS, J.J., QUAM, W.M. and GOODMAN, L.J. Composition of A-150 Tissue-Equivalent Plastic. *Med. Phys.*, 1977, 4(2), 74-77.

ALBERTS, W.G., DIETZ, E., GULDBAKKE, S., KLUGE, H. and SCHUHMACHER, H. *Radiation Protection Instruments Based on Tissue Equivalent Proportional Counters: Part II of an International Intercomparison.* PTB Report FMRB-117, 1988.

WAKER, A.J. and SOULIMAN, S.K. *Application of Tissue Equivalent Proportional Counters in Radiation Protection.* NPL Extramural Research Contract NPL-82-0429 Half-Yearly Report, September 1987.

STARK, M.S. and WAKER, A.J. *Application of Tissue Equivalent Proportional Counters in Radiation Protection.* NPL Extramural Research Contract NPL-82-0429 Half-Yearly Report, August 1986.

STARK, M.S. and WAKER, A.J. *Application of Tissue Equivalent Proportional Counters in Radiation Protection.* NPL Extramural Research Contract NPL-82-0429 Half-Yearly Report, November 1986.

THOMAS, D.J., CHARTIER, J.-L., KLEIN, H., NAISMITH, O.F., POSNY, F. and TAYLOR, G.C. Results of a Large Scale Neutron Intercomparison Exercise at the Cadarache Moderator Assembly. *Radiat. Prot. Dosim.*, 1997, 70(1-4), 313-322.

NAISMITH, O.F. and SIEBERT, B.R.L. A Database of Neutron Spectra, Instrument Response Functions, and Dosimetric Conversion Factors for Radiation Protection Applications. *Radiat. Prot. Dosim.*, 1997, 70(1-4), 241-245.

DAYHOFF, J.E. *Neural Network Architectures - An Introduction,* New York, Van

Nostrand Reinhold, 1990.

[30] SOULIMAN, S.K. and WAKER, A.J. *Application of Tissue Equivalent Proportional Counters in Radiation Protection.* NPL Extramural Research Contract NPL-82-0429 Half-Yearly Report, February 1988.

[31] WAKER, A.J. Principles of Experimental Microdosimetry. *Radiat. Prot. Dosim.*, 1995, 61(4), 297-308.

[32] TAYLOR, G.C. and THOMAS, D.J. *Neutron Scatter Characteristics of the Low-Scatter Facility of the Chadwick Building, NPL.* NPL report CIRM 17, 1998.

[33] NUNES, J.C. and WAKER, A.J. Multisphere Spectrometry and Analysis of TEPC and REM Meter Results Around a Heavy Water Moderated Reactor. *Radiat. Prot. Dosim.*, 1995, 59(4), 279-284.

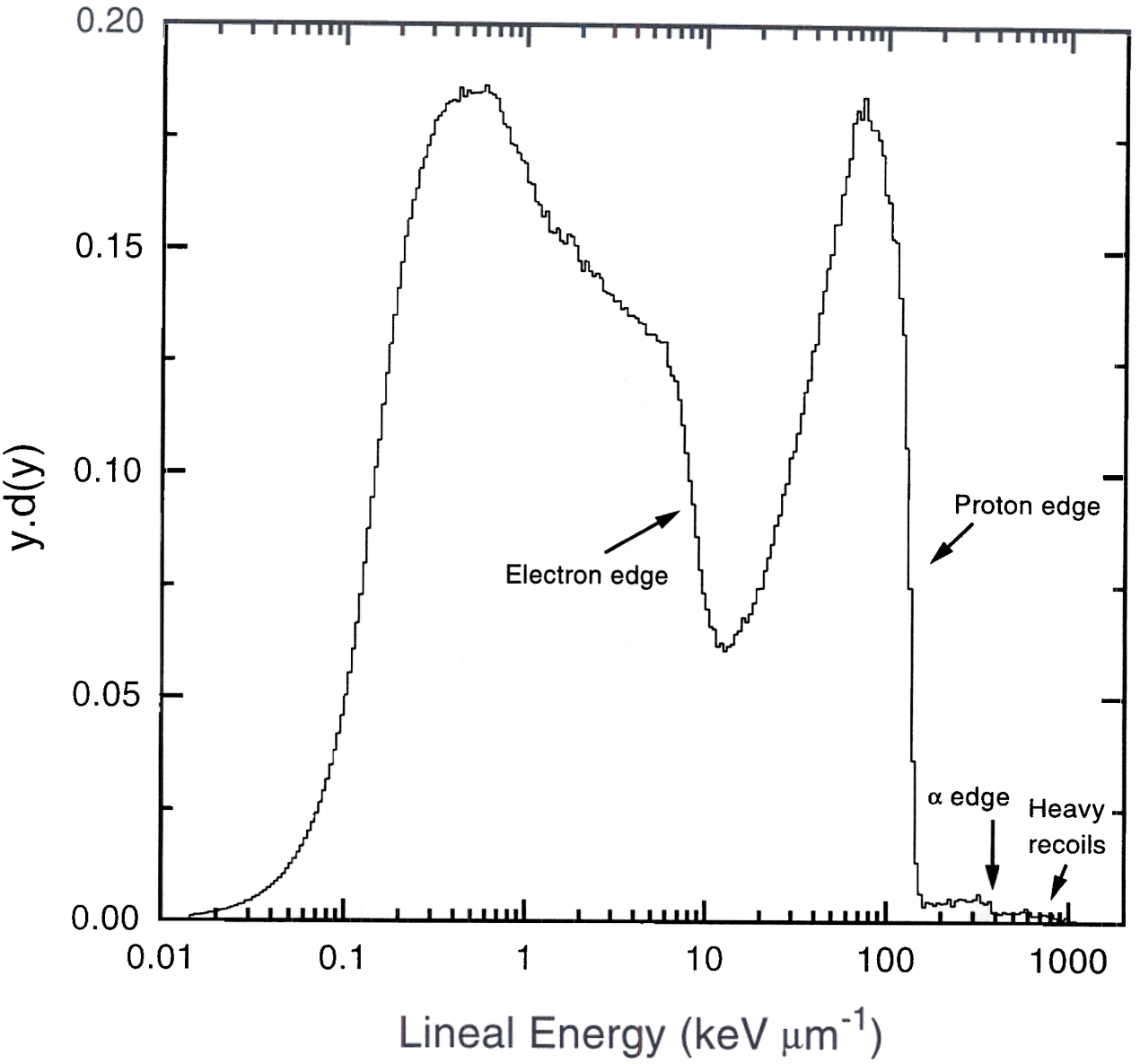

Figure 1. Microdosimetric spectrum measured at the Cadarache realistic field facility[27], showing features typical of a broad-range neutron spectrum.

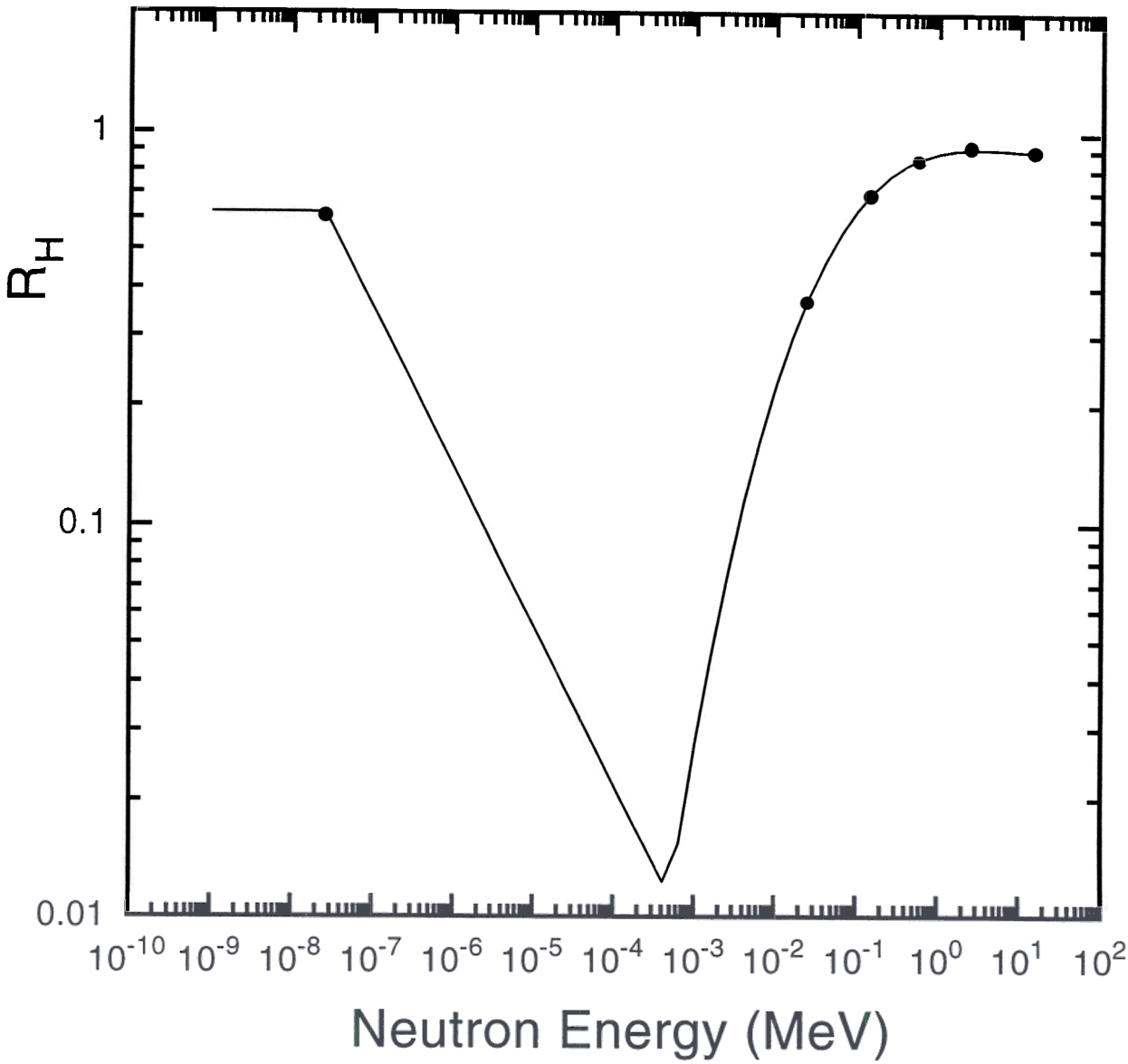

Figure 2. The performance of a 5" TEPC system in measuring the ambient dose equivalent as a function of neutron energy: analytical fit (———) to experimental data (•).
Taken from Nunes and Waker (1995)[33].

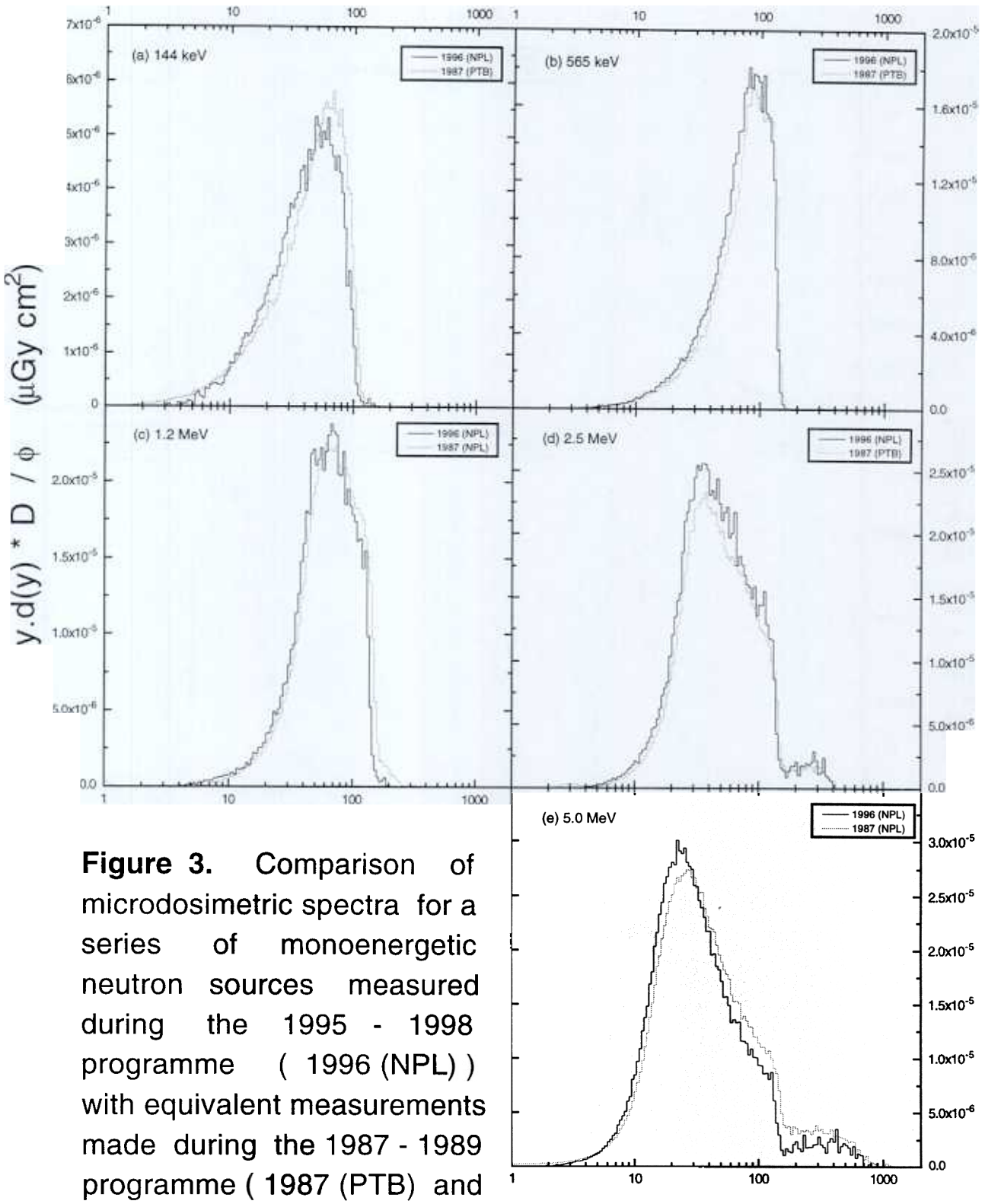

Figure 3. Comparison of microdosimetric spectra for a series of monoenergetic neutron sources measured during the 1995 - 1998 programme (1996 (NPL)) with equivalent measurements made during the 1987 - 1989 programme (1987 (PTB) and 1987 (NPL)).

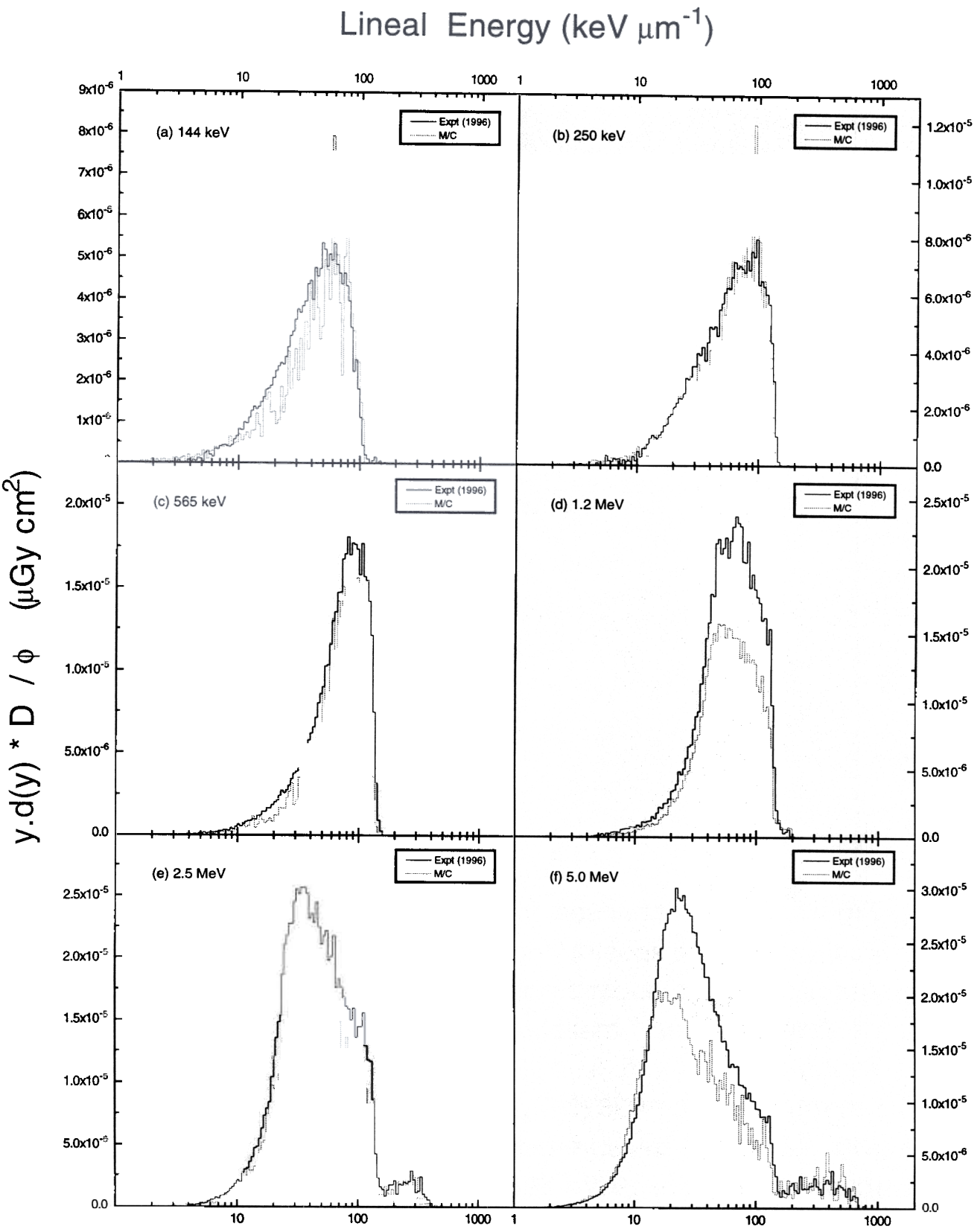

Figure 4. Comparison of microdosimetric spectra for a series of monoenergetic neutron sources measured during the 1995 - 1998 program with the MITE60 model using standard wall material.

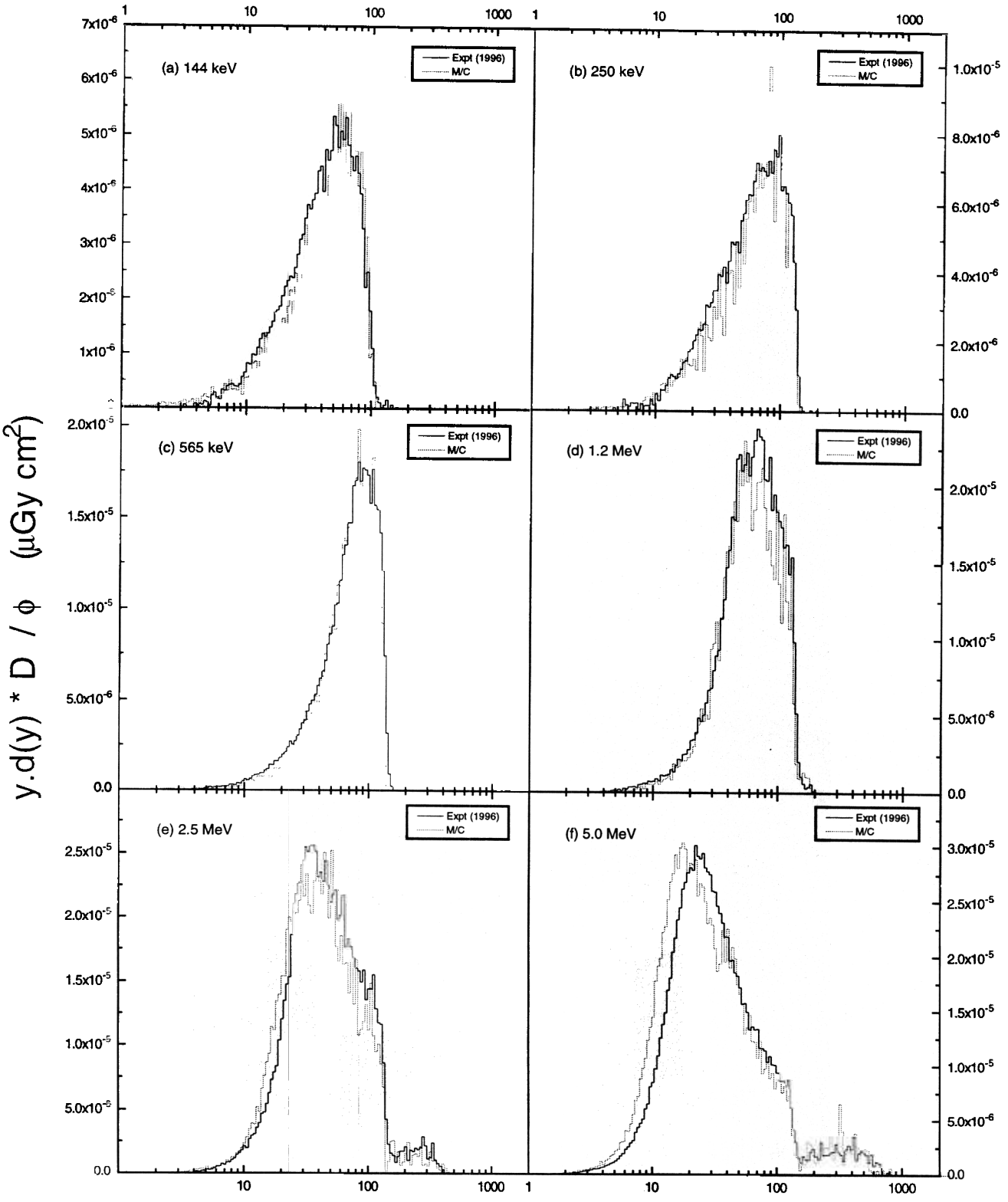

Figure 5. Comparison of microdosimetric spectra for a series of monoenergetic neutron sources measured during the 1995 - 1998 program with the MITE60 model using hydrogen-rich wall material.

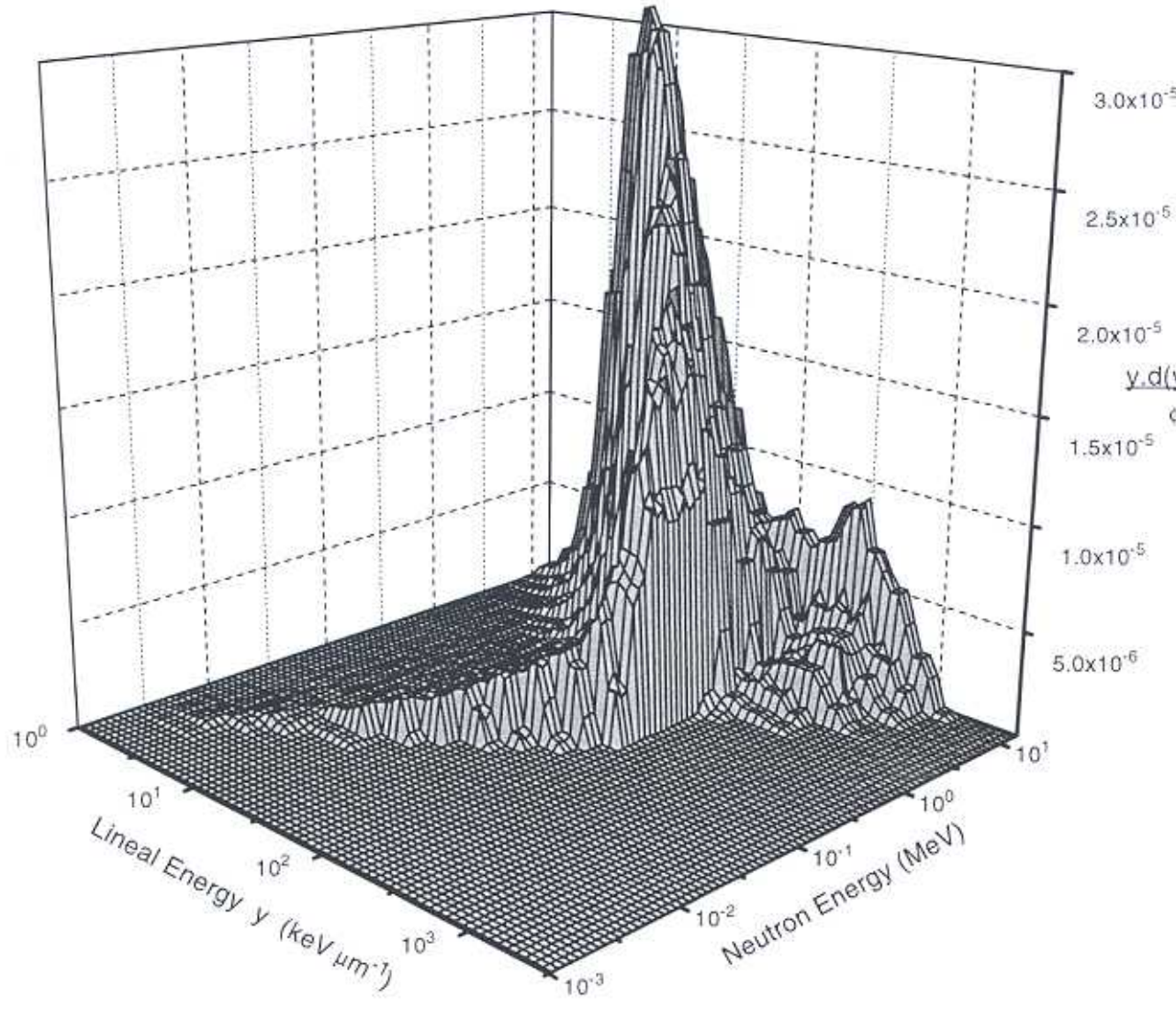

Figure 6. Three-dimensional plot of the variation in TEPC response with neutron energy. The plot only shows data for neutron energies greater than 1 keV as the absolute dose response below this energy is minimal.

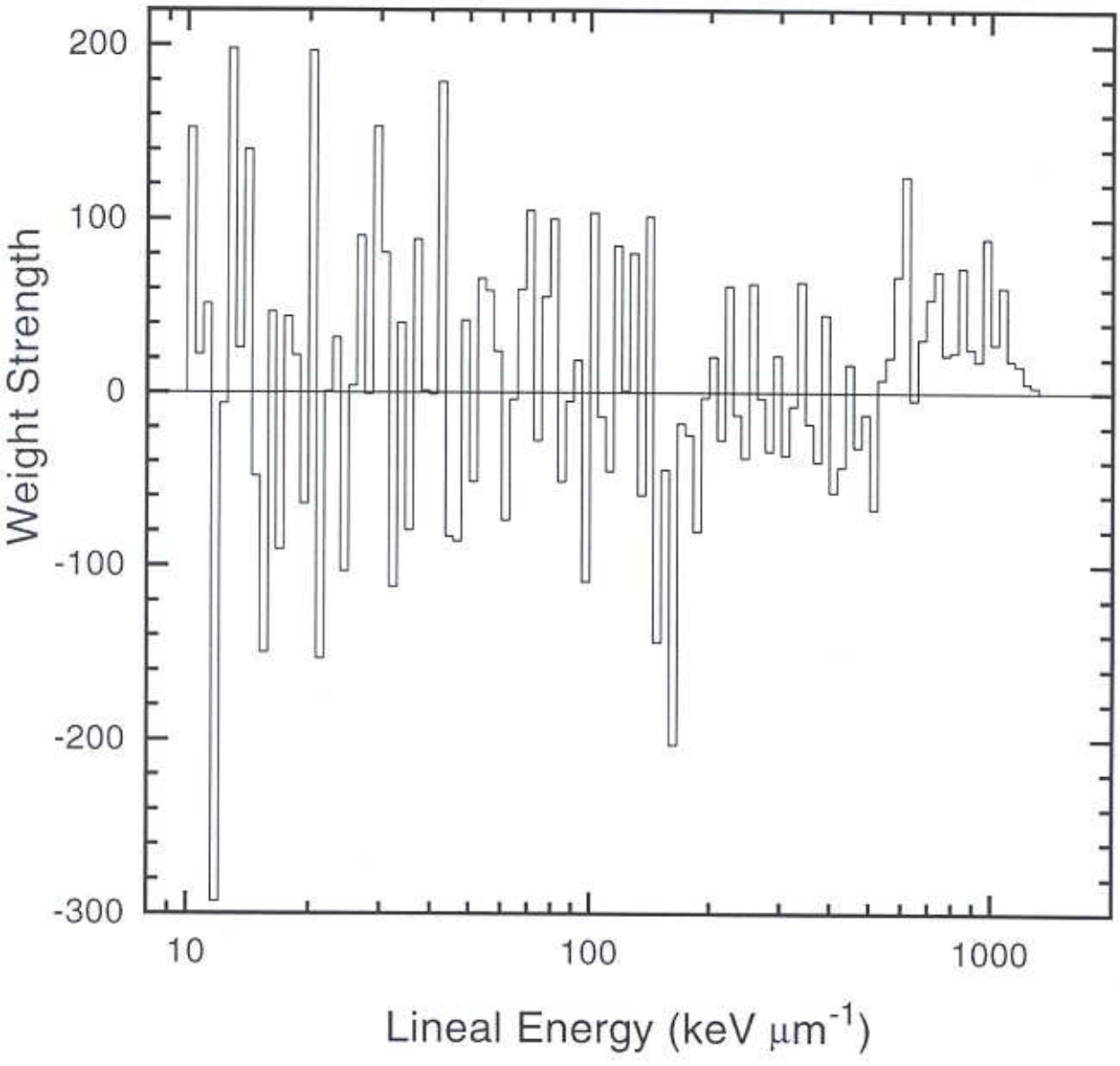

Figure 7. Strength of Weights in the Linear Neural Network

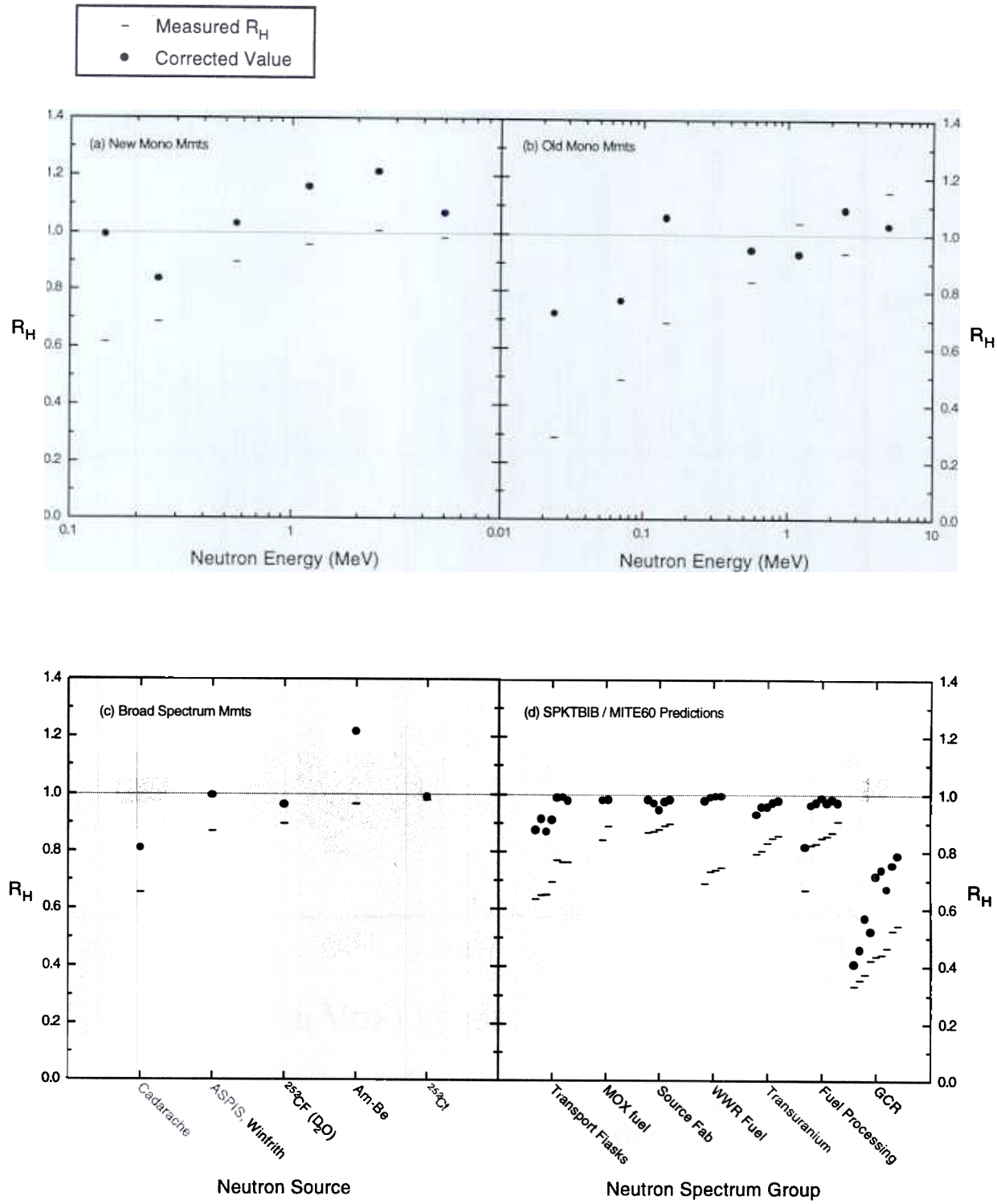

Figure 8. Effect of correcting the TEPC under-read using the Linear Neural Network

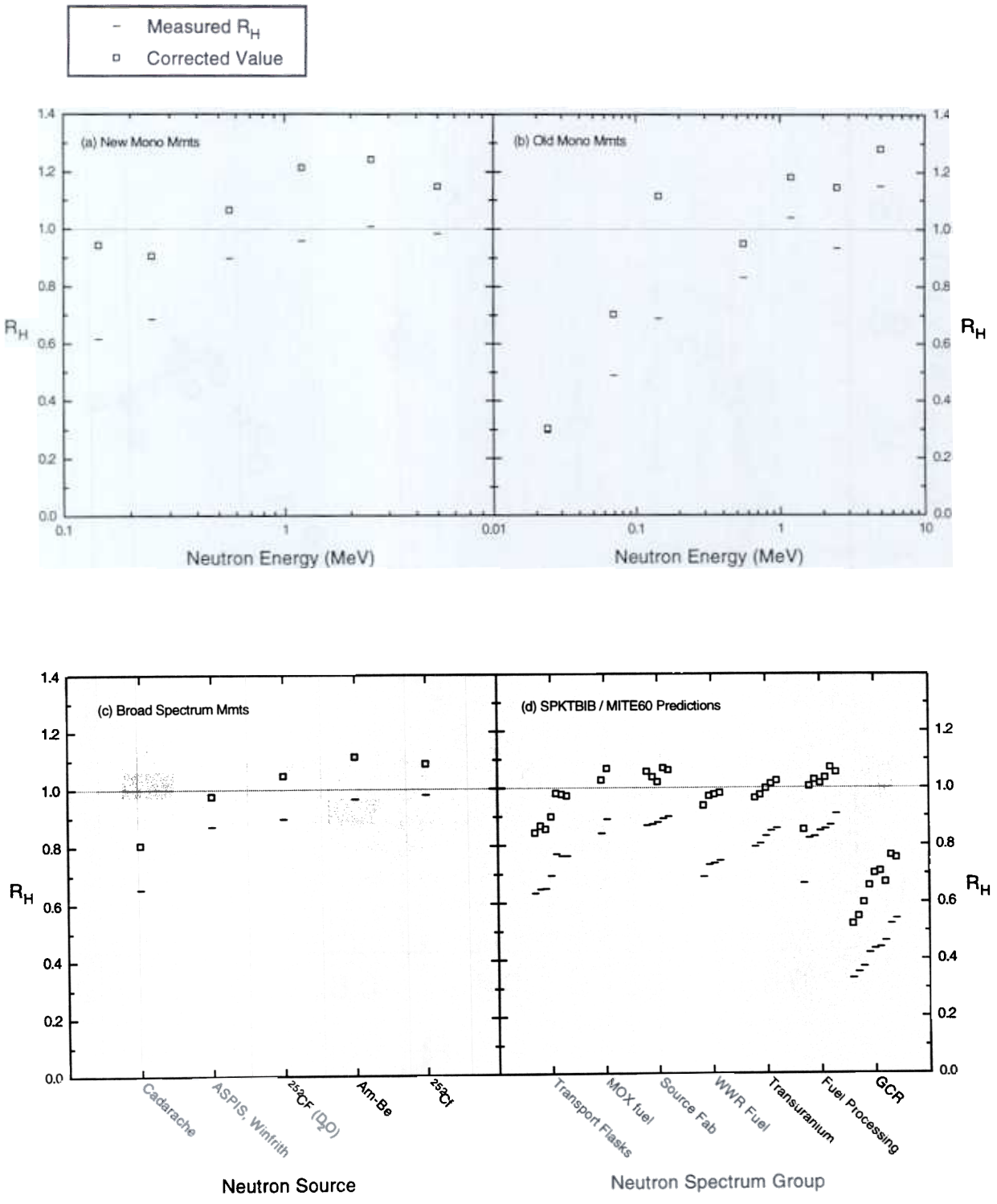

Figure 9. Effect of correcting the TEPC under-read using the Orthodox (Sigmoid) Neural Network

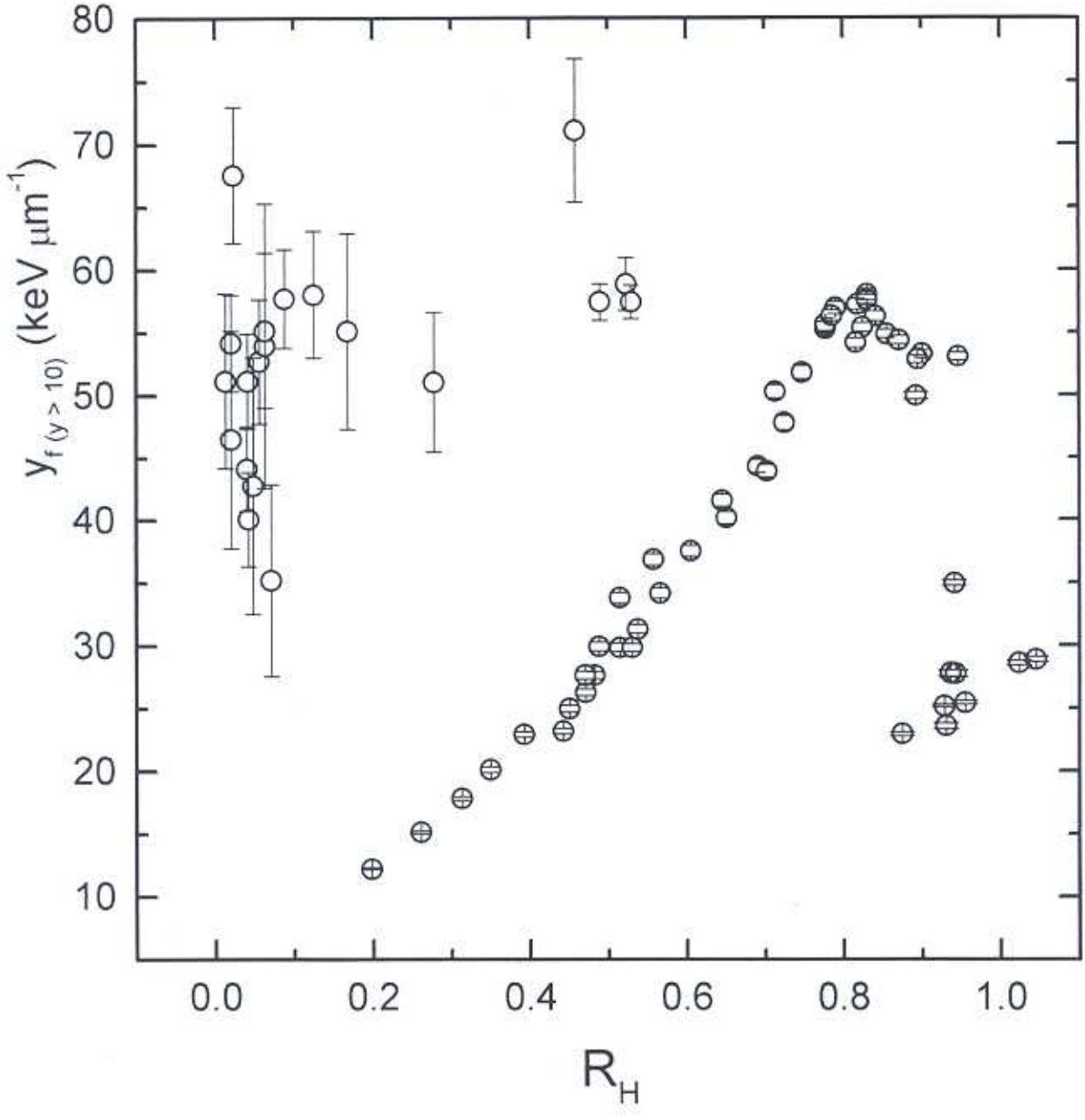

Figure 10. Variation in frequency-mean lineal energy for lineal energies greater than 10 keV μm^{-1} with ambient dose equivalent response.

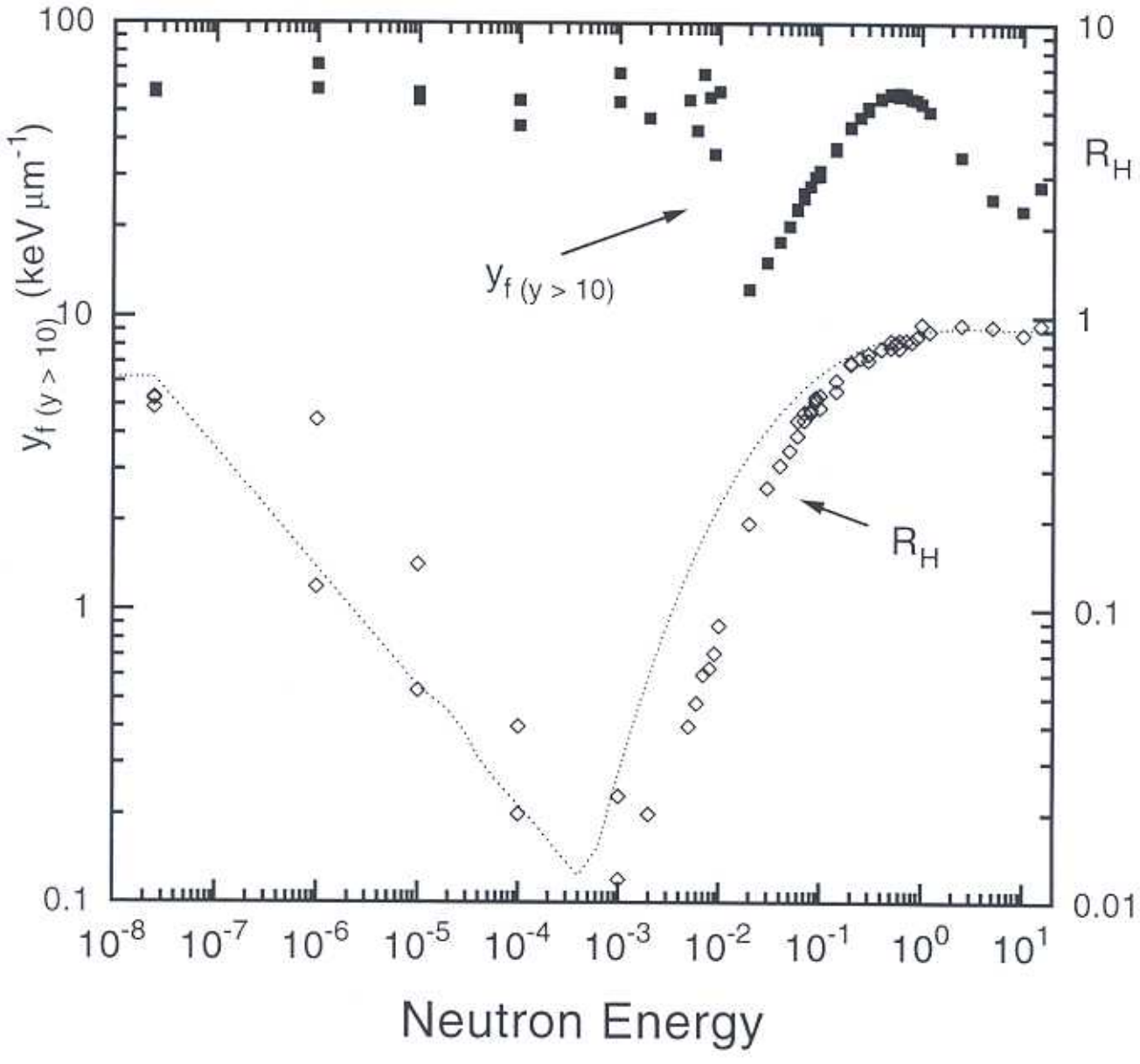

Figure 11. Relationship between the frequency-mean lineal energy for lineal energies over 10 keV μm^{-1} and the ambient dose equivalent response of the NPL 5" TEPC. Also shown is the R_H curve of Nunes and Waker from Figure 2 (·····).

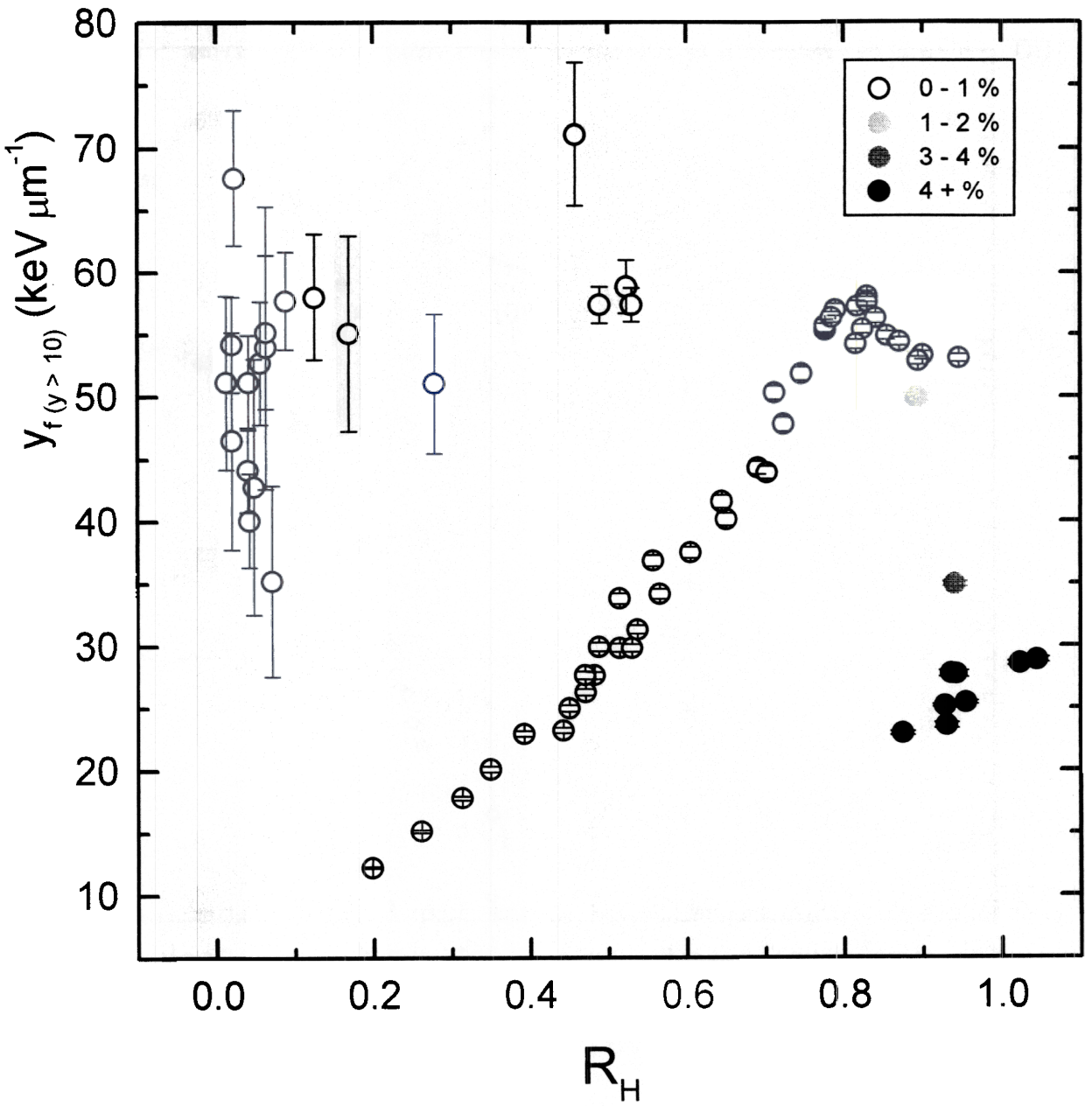

Figure 12. Variation in frequency-mean lineal energy for lineal energies greater than 10 keV μm^{-1} with ambient dose equivalent response. Also indicated is the dose fraction attributable to lineal energies greater than 136 keV μm^{-1}

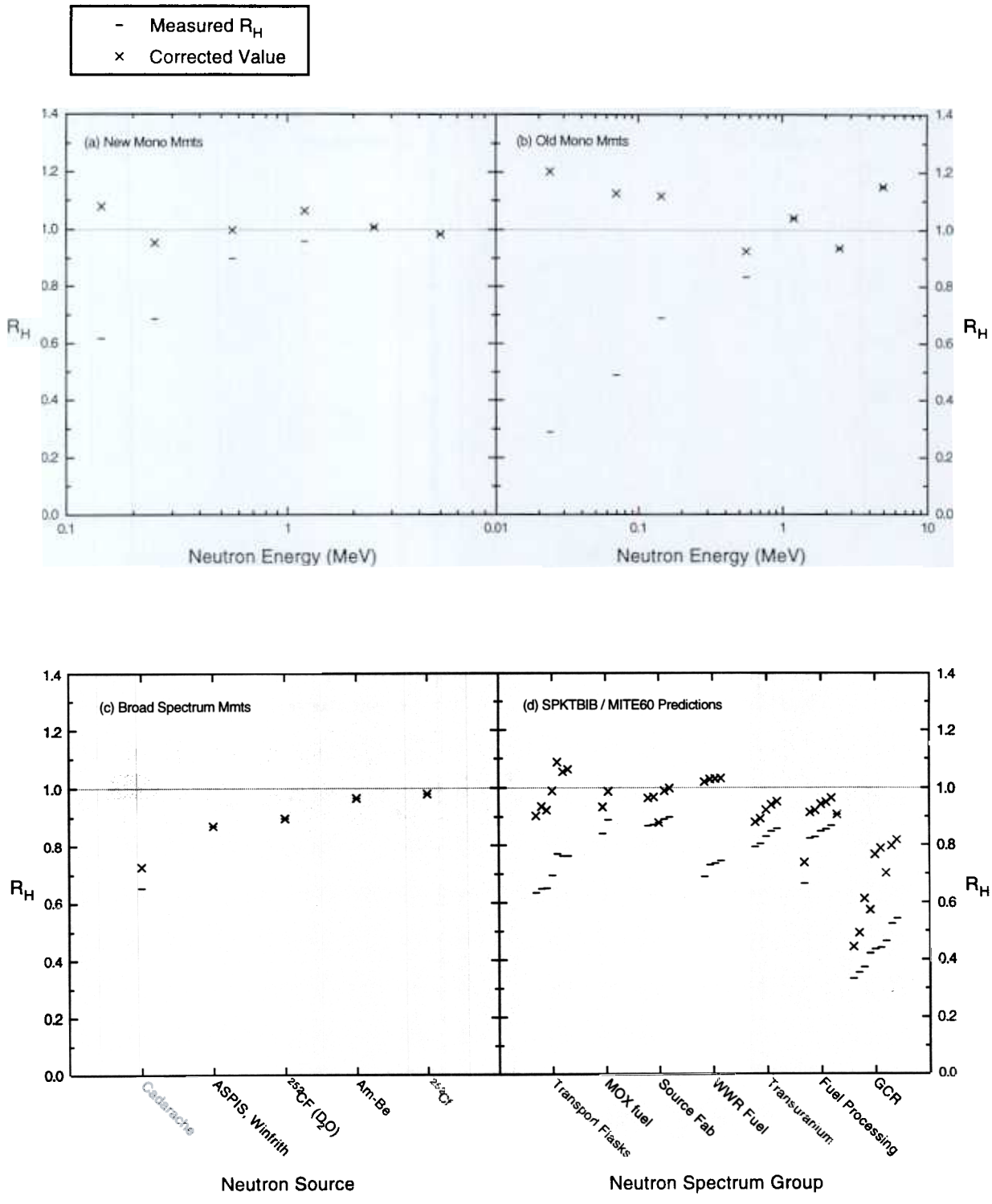

Figure 13. Effect of correcting the TEPC under-read using the mean value-matching technique.

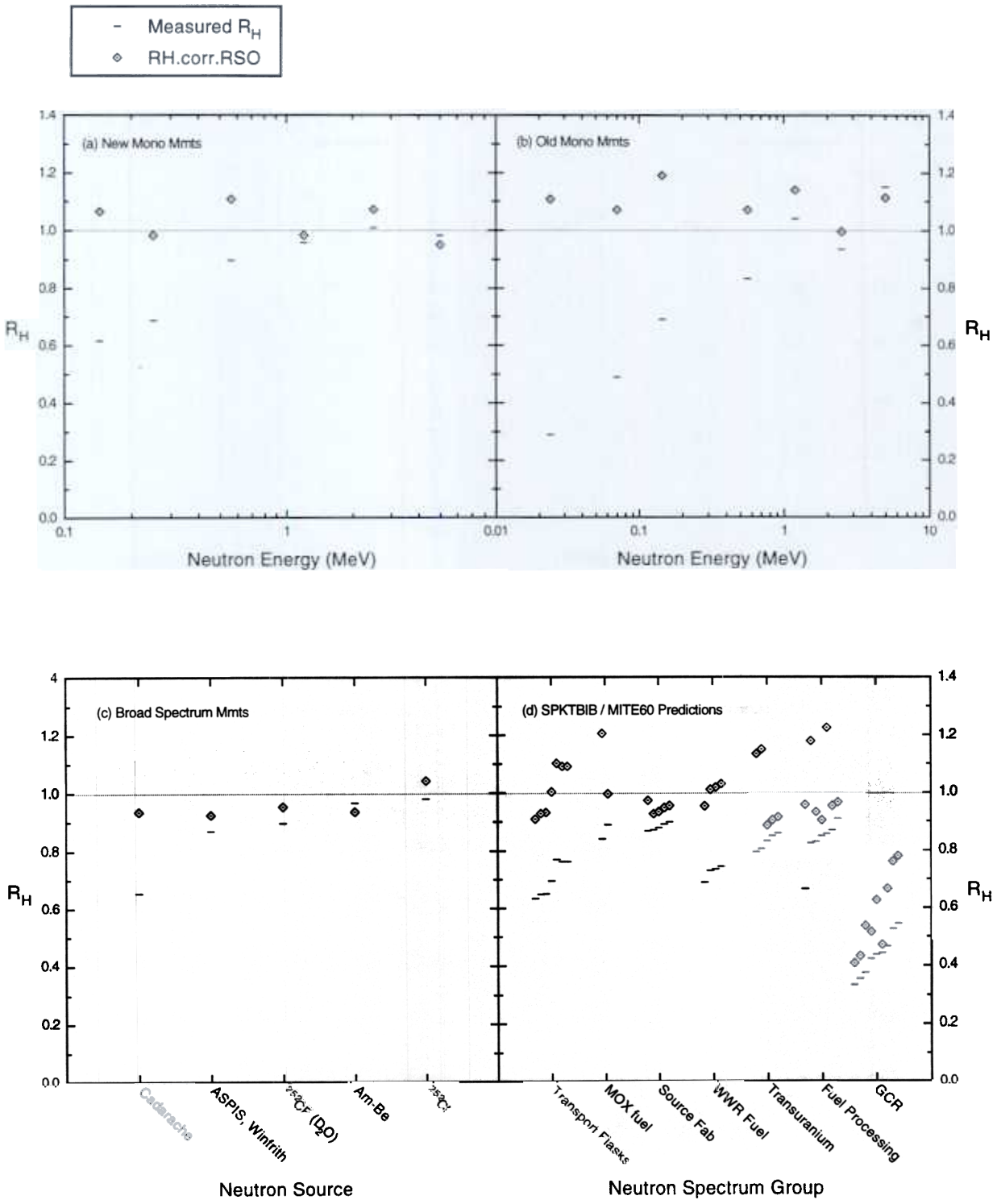

Figure 14. Effect of correcting the TEPC under-read using the spectrum-matching technique.

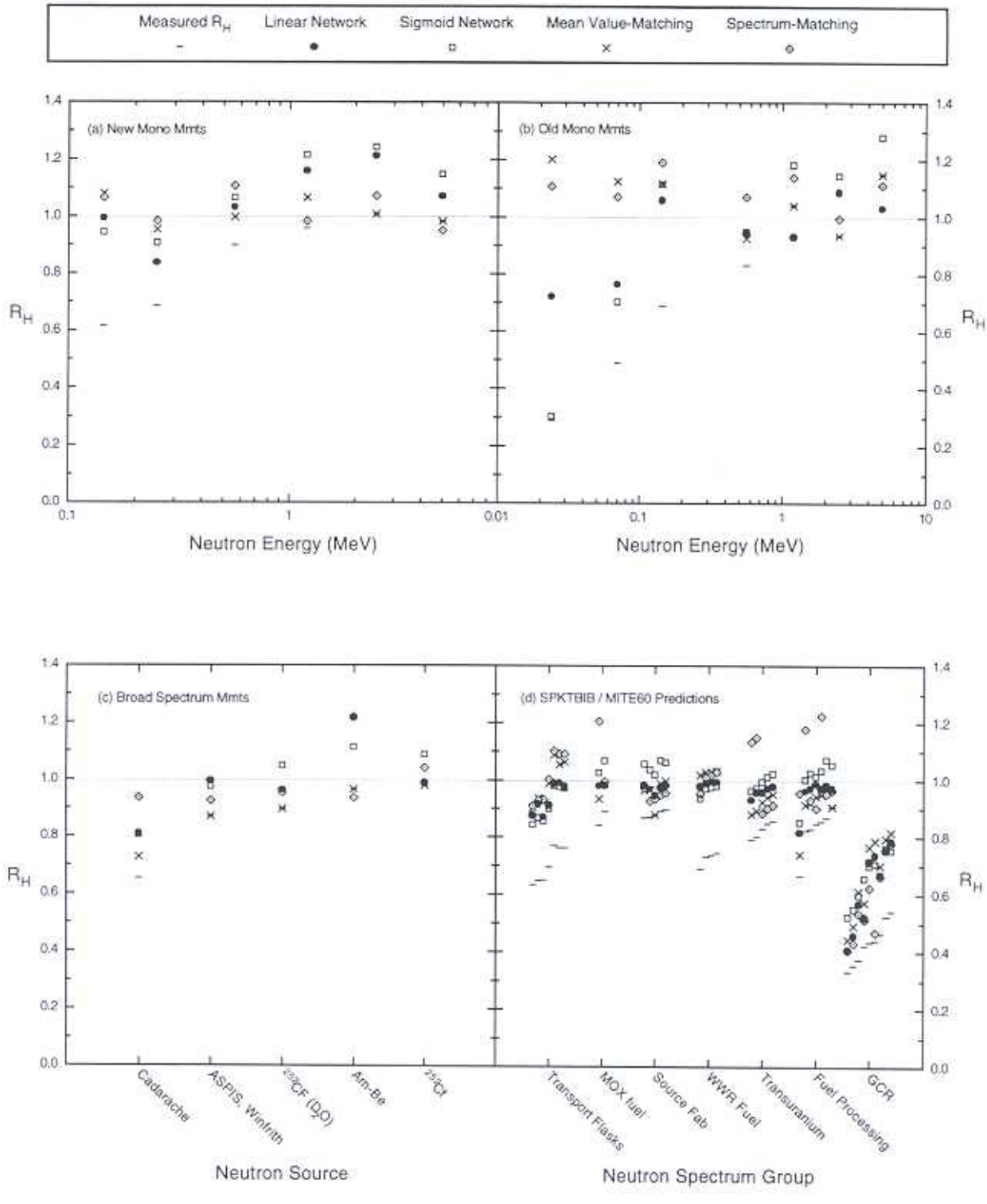

Figure 15. Comparison of all correction techniques